4. R.N. Coppolino and S. Rubin. Detectability of Structural Failures in Offshore Platforms by Ambient Vibration Monitoring. Proc., Offshore Technology Conference, Vol. 4, OTC 3865, May 1980, pp. 101-110.
5. I.E. Lindner. Dynamic Behavior of a Composite Highway Bridge. Univ. of Missouri-Columbia, Columbia, M.S. thesis, 1976.
6. R.K. Brady. An Experimental Study of the Dynamic Characteristics of a Composite Highway Bridge. Univ. of Missouri-Columbia, Columbia, M.S. thesis, Aug. 1977.

Publication of this paper sponsored by Committee on Dynamics and Field Testing of Bridges.

Fatigue Cracks and Their Detection

J.W. BALDWIN, JR., H.J. SALANE, AND R.C. DUFFIELD

A three-span continuous composite bridge of modern design was field tested under fatigue loading that produced stresses equal to or greater than design stresses. During the fatigue loading, a regular inspection schedule was carried out by using radiographic, ultrasonic, and visual methods. Ultrasonic inspection was the most reliable and, in the regions inspected regularly, no cracks are known to have grown to a length greater than 38 mm (1.5 in) before detection. Radiography was nearly as reliable as ultrasonic inspection where it could be used, but more than half the material to be inspected was inaccessible to radiography. A total of 18 fatigue cracks developed at the ends of welded cover plates and 2 fatigue cracks developed in base metal not adjacent to welds. At 471 000 cycles of loading, these cracks had propagated far enough to completely sever the girder flanges at five different sections. The fatigue life in regions where the stress range was 155 MPa (22.5 ksi) was considerably longer than would be predicted on the basis of current code requirements. However, the fatigue life in regions where the stress range was only 60 MPa (8.7 ksi) was considerably shorter than would be predicted on the basis of current code requirements.

During the past two decades, concern about the potential for fatigue failures in highway bridges has increased dramatically. Major laboratory studies have been carried out to determine load versus fatigue-life relationships and to establish design criteria (1,2). The design code of the American Association of State Highway Officials (AASHO) (3), which made little reference to fatigue considerations in the 1950s, now contains highly restrictive fatigue considerations that virtually eliminate certain types of construction. An intensive inspection program has been instituted by the Federal Highway Administration (FHWA) to evaluate the condition of bridges that were designed and constructed before fatigue was recognized as a serious problem.

Laboratory studies are by far the most efficient and cost-effective means of determining fundamental behavior modes in structures, but a certain amount of extrapolation is always required when design criteria for full-scale structures are developed from laboratory data. This is particularly true in the case of fatigue because fatigue behavior is highly sensitive to fabrication details, which are extremely difficult to model in scaled-down laboratory studies. Thus, an occasional check of design criteria through testing of full-scale structures under controlled loading conditions is highly desirable. An unusual opportunity to conduct such a test was created when flood-control work by the U.S. Army Corps of Engineers on the St. Francis River in southeast Missouri necessitated the removal of a 12-year-old highway bridge.

OBJECTIVES

The entire bridge was to be loaded cyclically at stress levels equal to or greater than service-load stresses until one or more girders failed. Objectives of the test were twofold. First, the fatigue behavior of the bridge was to be observed and compared with both laboratory results and current design criteria.

Before loading began and periodically during the test, the bridge was to be inspected by using several modern crack-detection techniques. The second objective, then, was to compare these techniques and to evaluate the effectiveness of each. This was to be the equivalent of inspecting a bridge every few years for its entire lifetime under normal service conditions. Since small cracks missed during one or more inspections would eventually grow into large cracks or failures, this procedure would provide information concerning sizes and types of cracks that are likely to be missed as well as those that are likely to be found.

DESCRIPTION OF TEST BRIDGE

The two-lane bridge was made up of three [21.9, 28.3, and 21.9 m (72, 93, and 72 ft)] continuous concrete-on-steel composite-girder spans. It was designed during early 1962 according to 1961 AASHO specifications for one H15-44 loaded lane. [For a general schematic of the bridge, see Figure 1 in Salane, Baldwin, and Duffield in this Record; see also the report by Salane and others (4).] Girders and cover plates were of American Society for Testing and Materials (ASTM) A36 steel, and the unshored slab was cast from concrete with a 28-day compressive strength of 36.6 MPa (5720 psi). Shear connectors were C4x5.4 channels 159 mm (6.25 in) long fillet-welded to the top flanges of the girders.

Channel diaphragms 460 mm (18 in) deep bent from 610x8-mm (24x0.31-in) plates were bolted to 114x9.5-mm (4.5x0.38-in) bearing stiffeners over the supports and to 76x9.5-mm (3x0.38-in) web stiffeners in the spans. There were two intermediate diaphragms in each end span and four intermediate diaphragms in the center span.

DESCRIPTION OF FATIGUE TEST

A total of 471 000 fatigue cycles were applied to the bridge over a period of approximately five weeks. Desired dynamic stress ranges were obtained by exciting the bridge at its first-bending-mode resonant frequency by using the closed-loop electrohydraulic shaker shown in Figure 1. This shaker consisted of 40 kN (9 kips) of steel weights attached to the top of an 89-kN (20-kip) servocon-

trolled hydraulic actuator that was bolted to the girders through the deck slab at the center of the bridge. During fatigue loading, approximately 178 kN (40 kips) of concrete ballast was anchored to the deck slab at the center of each span. This ballast produced a mean stress on which the cyclic stress was superimposed so as to produce a loading similar to the application and removal of load under service conditions.

Strain gauges were located on the top and bottom flanges of each girder at seven sections along the bridge as illustrated in Figure 2. Since these sections were critical in the girders, both strain-gauge locations and section locations were designated in terms of the section numbers and girder numbers shown in Figure 2. A designation of 2.4B means section 2, girder 4 (north exterior girder), bottom flange.

Additional instrumentation included deflection gauges at the centers of all spans, gauges to measure slip between the slab and the girders, and accelerometers at several locations. All strain and deflection gauges were read and recorded automatically either on punched paper tape by using a peak detector and a 100-channel scanner or on magnetic tape by using a high-speed analog-to-digital converter.

Prior to the start of fatigue loading, the bridge was thoroughly inspected for cracks by using all the techniques except dye penetrant. During fatigue loading, the test was stopped periodically for inspection by the various crack-detection techniques. Inspection intervals varied from approximately 20 000 to 60 000 cycles depending on the degree of cracking activity that was occurring at the time. It was possible to conduct visual and some ultrasonic inspection while fatigue loading was being applied, and these observations were used as a guide in selecting the times at which the test should be stopped for complete inspection. A complete description of the test procedure has been presented by Baldwin, Salane, and Duffield (5).

Figure 1. Electrohydraulic shaker.

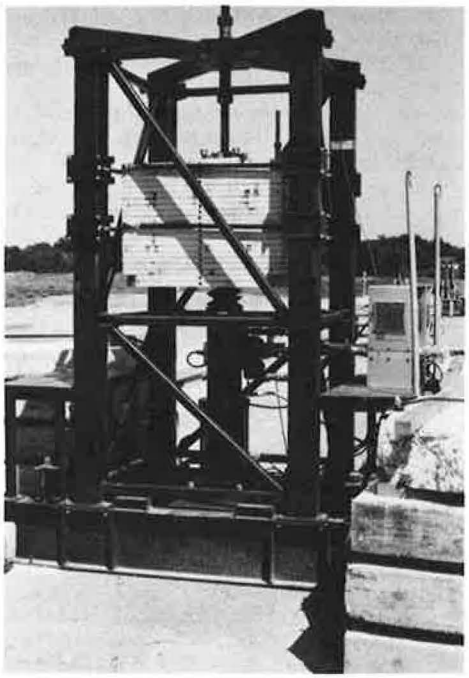

FATIGUE CRACKS

Ultrasonic inspection prior to loading revealed only one detectable flaw, and follow-up inspections during the test indicated that this flaw did not develop into a crack. The feasibility study for the project indicated that the critical regions for fatigue cracking would be at the ends of the bottom-flange cover plates in the end spans, gauge sections 2 and 6.

Bottom-Flange Critical Section

Nominal stresses at these sections, including dead load, ballast, and dynamic load, were from approximately 138 MPa (20 ksi) compression to 17 MPa (2.5 ksi) tension, or a stress range of 155 MPa (22.5 ksi). Variations from girder to girder were approximately ±10 percent from these values.

Figure 2. Strain-gauge locations.

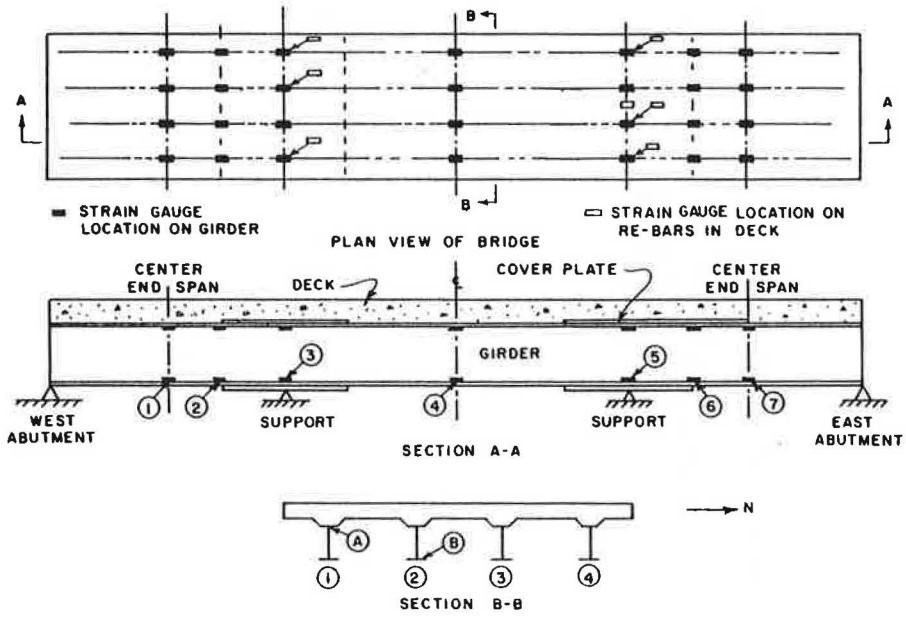

During the inspection at the end of 19 500 cycles of load, cracks of the order of 6.4 mm (0.25 in) length were detected ultrasonically in five of the eight critical flange regions. After 287 000 fatigue cycles, cracks had been detected in all eight of these critical regions. These cracks did not initiate at the toe of the weld as might have been expected but started at the root or heel of the weld at some point across the end of the cover plate as shown in Figure 3. These cracks did not enter the girder flange at this point but propagated along the fusion line to the surface of the weld and across the end of the cover plates. In most cases, they turned the corner of the cover plate and proceeded along the beveled edge until at some point the crack turned into the weld metal propagating perpendicular to the axis of the beam (Figure 4). Once the cracks had entered the weld material, they continued through it into the base metal of the bottom flange and continued to grow in the typical semielliptical pattern. In five of the eight critical flange regions, the cracks propagated into the base metal on both sides of the cover plate, which resulted in two separate cracks in the base metal (Figure 5).

Figure 3. Crack initiation at heel of weld.

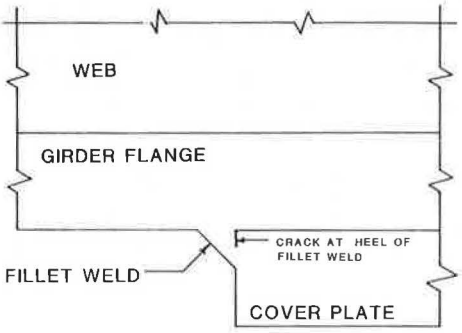

Figure 4. Crack propagation.

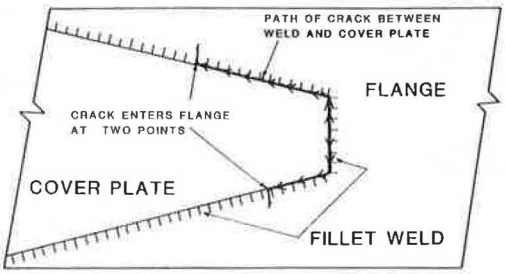

Figure 5. Cross section of flange showing two fatigue cracks.

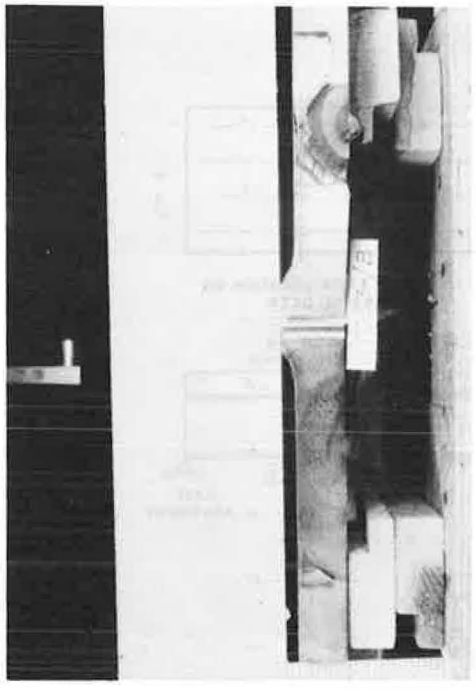

In all there are 13 separate cracks that entered the base material of the bottom flanges at the ends of cover plates. Two of these cracks, located at section 6.1B, propagated to failure and completely severed the bottom flange at 455 000 fatigue cycles. The crack on the south side at section 2.2B propagated to a total length of 90 mm (3.5 in) at 438 000 cycles but showed no perceptible additional growth beyond that point (Figure 5). No growth was observed in any of the other 10 cracks beyond approximately 415 000 fatigue cycles.

In the design of ductile structures subjected to static loads, it is normal practice to consider stresses that result from directly applied loads and neglect "locked-in" stresses such as cooling residual stresses and erection stresses. Under static loading, these locked-in stresses are dissipated by local yielding with very little effect on the general behavior of the structure. Fatigue-crack growth, however, is governed by the actual stress cycles in the zone around the tip of the crack, and locked-in stresses are superimposed on the nominal stress cycle in this zone. Thus the actual stress cycle has the same stress range as the nominal cycle but a significantly different mean stress.

It is reasonable to assume that the test bridge contained tensile residual stresses equal to the yield point in regions of the flanges in which fatigue cracks entered the base metal from the weld. Consideration of these residual stresses results in the stress-cycle pattern shown in Figure 6. Both dead load of the slab and ballast loads produced compression in the bottom-flange critical sections that reduced the total stress at the crack-initiation points from the yield point of 262 MPa (38 ksi) to 202 MPa (29.25 ksi). The cyclic dynamic load was then superimposed on this mean stress and as the amplitude built up to $\pm$77.6 MPa (11.25 ksi), the maximum stress again reached the yield point, which caused local yielding. This yielding relieved part of the residual stress, which in turn lowered the mean stress.

Mean stress at the crack tip then remained constant and maximum stress reached the yield point on each cycle as the crack propagated through the tensile-residual-stress zone. As the crack propagated from the tensile-residual-stress region into the region of zero residual stress, the mean stress decreased to -60 MPa (-8.75 ksi), the sum of dead load and ballast stresses.

A total of 13 cracks propagated in the tensile-residual-stress zones where the mean stress was 202 MPa, but even though the stress range remained constant, all except one of these cracks stopped growing when the mean stress dropped to -60 MPa. This suggests that mean stress at the tip of the crack must be significant in at least those cases in which part of the stress cycle is in compression.

This observation is consistent with a fracture-mechanics analysis if it is assumed that fatigue-crack growth is governed primarily by the stress-intensity range ΔK_I. The general form of the equation for computing K_I is as follows:

Figure 6. Fatigue stress cycles.

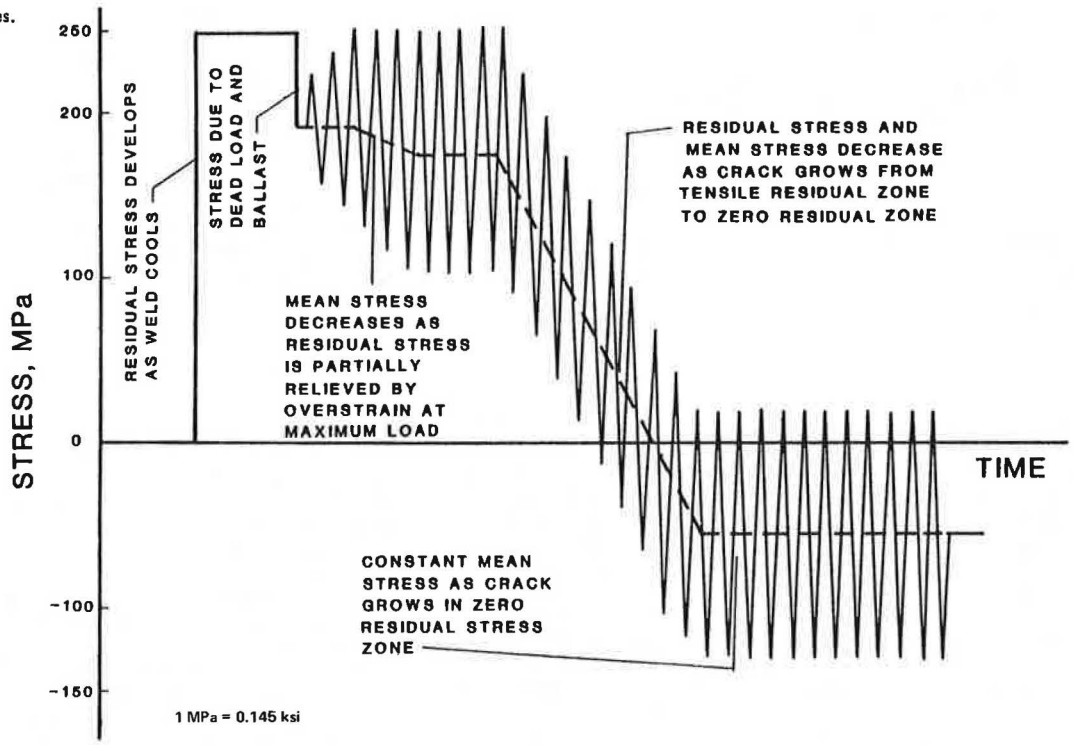

$$K_I = C\sigma\sqrt{a} \quad (1)$$

where C is a constant dependent on the geometry of the member and type of crack, σ is the nominal stress, and a is the crack length. This equation is derived from an elastic analysis of the stress field around the crack tip and is based on the assumption that no stress is transmitted across the crack. As long as the entire stress range in the vicinity of the crack is in tension, the following holds:

$$\Delta K_I = C\Delta\sigma\sqrt{a} \quad (2)$$

and the mean stress does not enter into the analysis. However, if the mean stress is such that compressive stress is transmitted across the crack during part of the cycle, Equation 1 becomes invalid during that part of the cycle. In fact, there is probably very little change in the stress intensity during that part of the cycle when the crack is closed.

The foregoing analysis does not account for the possibility of erection stresses or stresses that arise from differential settlement. Such stresses could be either tensile or compressive, could vary from girder to girder, and are impossible to estimate accurately. If they were tensile, they would cause immediate local yielding and no increase of total stress in regions where initial tensile residual stresses were already to the yield point.

The total stress would remain at the tensile yield point and stress cycles would be unaltered during crack initiation and growth through the tensile-residual-stress zone. Once the crack tip reached the zero-residual-stress region, presence of tensile erection or settlement stress would raise the mean stress above the level shown in Figure 6 by an amount equal to the erection or settlement stress.

Erection or settlement stresses algebraically less than -17 MPa (-2.5 ksi) would lower the entire stress pattern and force the complete stress cycle into the compression zone before the crack tip reached the region of zero residual stress. Stresses of this type could easily account for variations in the lengths at which crack growth was arrested in different sections.

Top-Flange Critical Sections

Calculations during the feasibility study indicated that stress ranges at the ends of the top-flange cover plates in the end spans, gauge sections 2 and 6, would be 90-97 MPa (13-14 ksi) and that there was the possibility of failure before 500 000 cycles. The initial test plan therefore called for continuous ultrasonic monitoring of these regions.

Once the test load was under way, strain measurements indicated that there was considerably more composite action at these critical sections than had been assumed during the feasibility study. Nominal stresses under test loading were from approximately 41 to 101 MPa (6.0-14.7 ksi) tension, which produced an average stress range of only 60 MPa (8.7 ksi). Both the AASHO specifications and previous research results presented by Fisher indicated a fatigue life of nearly 2 million cycles under this low stress range. Because of this and the fact that ultrasonic testing was the critical activity in a very tight testing schedule, ultrasonic monitoring of the top flanges was discontinued.

However, at 415 000 fatigue cycles, a routine visual inspection of the bridge revealed that cracks approximately 150 mm (6 in) long had developed in the top flanges of girder 1 at section 2 and girder 2 at section 6. Ultrasonic monitoring of the top flanges at sections 2 and 6 was immediately reinstated, but no additional cracks in top flanges were detected during the tests. The cracks in girder 1 at section 2 and girder 2 at section 6 propagated to failure, completely severing the flanges at 453 000 and 462 000 cycles, respectively. After completion of the fatigue test, the slab was removed and cracks in the welds at the ends of the cover plates were detected by using dye penetrant at sections 2.1A, 2.3A, and 6.1A.

The fact that two of the eight sections subjected

Figure 7. Detail of top-flange critical section.

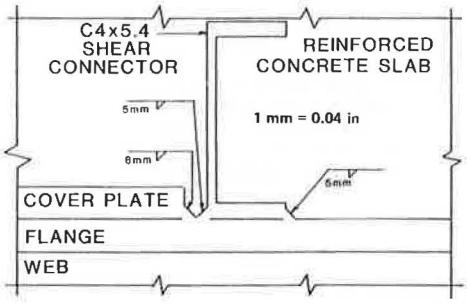

to essentially the same loading failed at less than 25 percent of the cycles permitted by the current code is reason for concern. In addition to the magnitude of stress range, there were two primary differences between these top-flange critical sections and the bottom flanges immediately below them. In the top flanges, the nominal stress range was entirely in the tension region; the maximum tensile stress was 101 MPa (14.7 ksi), whereas the nominal stress range in the bottom flanges was primarily in the compression region and the maximum tensile stress was only 17 MPa (2.5 ksi). The other difference was the particularly severe weld detail in the top flange. A channel shear connector had been fillet-welded to the base metal of the top flange adjacent to the end of the cover plate so that the two fillet welds were toe to toe and slightly overlapped (Figure 7).

In the vicinity of the welds where the cracks began, any effect of the difference in maximum nominal stresses between the top and bottom flanges would have been negated by the fact that tensile residual stresses would have raised the maximum stress at the crack tip to the yield point in both cases. Thus, any differences in crack initiation between the top and bottom flanges must have been due to differences in stress range and detail. It is clear that the stress range in the top flange was not great enough to initiate cracks in the same way that they were initiated in the bottom flanges. The five cracks that did begin in the top flanges all started at the intersection of the two fillet welds. The fact that two of the cracks started much earlier than the other three and that there were three top flanges in which no cracks were detected suggests that there were significant differences in the severities of flaws in these regions. At section 6.2A there was a 5-mm (0.19-in) slag inclusion that apparently initiated the crack. Unfortunately, the nearly two years that elapsed between the end of the fatigue test and demolition of the bridge deck permitted severe corrosion of the fracture surfaces, and attempts to identify the point of crack initiation at section 2.1A were unsuccessful.

Because the only top-flange cracks that grew significantly were quite large before they were detected, it is difficult to draw conclusions regarding the growth rates of these cracks. However, the fatigue lives of the top flanges that did develop cracks early were rather short for the stress range involved. This would have been influenced some by the size of the flaws that initiated the cracks. It was also undoubtedly influenced considerably by the length of the zone of high residual tensile stress. The geometry of the weld detail was such that these cracks would have grown in the zone of high tensile stress in which the maximum stress at the crack tip was equal to the yield point for more than one third of the width of the flange.

At 415 000 fatigue cycles, cracks at sections 6.2A, 2.1A, and 6.1B were all approximately the same length. Even though the stress range at section 6.1B was 2.5 times those at the other two sections, the first failure was 2.1A and all three sections failed within a 9000-cycle period. During the period from 415 000 cycles to failure, all three cracks were growing in regions of base metal in which there was probably little or no residual stress and little influence from weld details. Thus, the growth rate at section 6.1B must have been retarded by the fact that much of the stress cycle was in compression.

Center Span

At 373 500 fatigue cycles, the bottom flange at girder 2 failed with a loud bang at the center of the center span. Although the stress cycles at this section were from essentially nothing to 223 MPa (32.3 ksi), there were no welds on the flange, and base metal at a stress range of 223 MPa would not be expected to fail until more than 1.25 million fatigue cycles had been applied. Examination of the fracture revealed that a fatigue crack had started at a heat number stamped on the face of the bottom flange (Figure 8).

A piece of the beam around the fracture was cut out for laboratory examination and a bolted splice applied so that the test could continue. At 470 700 fatigue cycles, this girder fractured again at another heat number about 102 mm (4 in) from the end of the splice. Although girder 2 suffered two fractures, no cracks were detected in the girders on either side of this girder even though they were both subjected to the same stress conditions and were also heat-stamped on the face of the bottom flange. Girder 2 was from a different heat of steel than the girders on either side, which led to speculation that there was a difference in the fatigue resistance of these two levels of heat. However, subsequent tests of material cut from these three girders have shown no significant differences in material properties. Thus, the difference appears to have been in the sharpness of the heat-stamp dies.

CRACK-DETECTION METHODS

Ultrasonics

During the course of the fatigue test, a total of 17 inspections were conducted by using a conventional pulse-echo ultrasonic unit. For crack detection, the transducer was a 5-MHz 45-degree transceiver probe. For the initial inspection, a 5-MHz 90-degree split-crystal probe was also used to locate the channel shear connectors, which were welded to the top of the top flange and embedded in the slab.

The initial inspection was conducted before testing started and included complete inspection of both the top and bottom flanges at the ends of the cover plates in both the end and center spans. This initial inspection also included locating and marking the ends of the cover plates and shear connectors on the top flanges. The only flaw detected during this inspection was in the fillet weld at the end of the top-flange cover plate on girder 3 at section 6. However, this flaw did not develop into a crack and there was no noticeable change in the flaw during the entire test.

Because bad weather had forced a very condensed testing schedule and ultrasonic inspection proved to be quite time consuming, subsequent inspections were in general limited to the critical regions of the bottom flanges around the ends of the cover plates in the end spans. The second inspection was con-

Figure 8. Fatigue crack initiated by heat stamp.

ducted after 19 530 fatigue cycles. A total of six cracks each approximately 6.4 mm (0.25 in) long were discovered during this inspection. In every case, the ultrasonics clearly indicated that the crack was not at the toe of the weld, as might be expected, but rather at the heel of the weld.

At 95 000 cycles, a total of 10 cracks had been detected ultrasonically, but it was not until 202 000 fatigue cycles that any of these cracks were seen on the surface. Even then they could be seen only with the aid of a dye penetrant. Visual observations by using dye penetrant indicated that in some cases the crack in the weld was considerably longer than indicated by the ultrasonic measurement. This was due at least in part to the fact that without special techniques there is an ultrasonic blind spot directly below the web of the beam. In many cases in which two cracks were recorded, one on either side of the web, they were actually connected through this blind spot and formed a single crack.

All these cracks were monitored for the remainder of the test, and a complete record of crack lengths as measured ultrasonically is presented in Table 1. In those cases in which the cracks propagated across the entire width of the flange, it was possible to trace their growth ultrasonically to within approximately 2.5 mm (0.1 in) of the edge before the crack became visible on the edge.

After completion of the test, two sections that each contained two cracks that had stopped during the test were cut from the bridge and separated in the laboratory. It was then possible to compare the actual lengths of these four cracks with the lengths indicated by ultrasonic measurements. For two of the cracks the ultrasonic measurements were essentially correct. One ultrasonic measurement was in error by 6.4 mm (0.25 in) and the other by 10 mm (0.4 in).

For the critical regions at the ends of the cover plates on the bottom flanges, the conventional pulse-echo ultrasonic unit proved to be quite reliable in finding fatigue cracks under field conditions. All cracks that grew large enough to be detected visually had previously been detected ultrasonically when they were less than 38 mm (1.5 in) long and 60 percent of them were detected at a length of 6.4 mm.

Ultrasonic inspection of the critical regions at the ends of cover plates on the top flanges was not so successful. Because stress ranges were low in the top flanges, ultrasonic inspection was discontinued early in the test and was not resumed until two cracks had been observed visually. Of course, the failure to detect these two cracks ultrasonically cannot be interpreted as an adverse reflection on the capability of the ultrasonic inspection because no attempt was made to detect them. However, subsequent ultrasonic inspections of the other six critical top-flange regions that were subjected to essentially the same stress histories revealed no additional cracking. The cracks that were detected by using dye penetrant subsequent to removal of the deck were missed completely by the ultrasonic inspection. Examination of the geometry of the detail at this joint indicates that it is very difficult to detect cracking at the toe of the fillet weld, as shown in Figure 9. Under ideal conditions the surface of a crack is sometimes rough enough to reflect a signal directly back to the transducer even though the angle of incidence is other than zero, but under field conditions in which the transducer must be acoustically coupled through a painted surface that tends to be rough or irregular, it is almost essential that the signal be reflected either by a surface perpendicular to the ultrasonic beam or by doubling a corner if it is to be strong enough for detection. Thus, there is serious doubt about the reliability of conventional ultrasonic inspection to detect cracks in a detail of this type.

Two undetected cracks developed and grew to complete failure in girder 2 near the center line of the bridge. Since cracking was not expected in this region, there had been no ultrasonic inspection prior to development of the first crack. Immediately after the first crack developed, the entire area was scanned ultrasonically but no additional cracks were detected. Although there was frequent monitoring of this region during the remaining 93 000 cycles of the test, no additional cracks were detected ultrasonically and the final failure was by sudden fracture of girder 2 approximately 1 m (3 ft) from the first fracture. The cracks leading to both these fractures had initiated at heat numbers stamped into the flange. After the test loading had been stopped, these regions were again examined very carefully by using the ultrasonic probe, but no cracks were detected.

Dye Penetrant

Once the ultrasonic inspection indicated that cracks in the weld were 12.7 mm (0.5 in) or more in length, repeated attempts were made to observe these cracks visually at the surface. When these attempts failed, a dye penetrant was introduced to enhance the visibility of the cracks. These attempts were also unsuccessful until the paint was removed from the area to be inspected. However, once the surface was free of paint, the dye penetrant gave a vivid indication of cracks that were previously invisible to the unaided eye. By reapplying the dye penetrant periodically, it was quite easy to trace the progress of crack growth during the remainder of the test.

Since dye penetrant is quite easy to apply and interpretation of the results requires no special training or skill, it would seem to be an excellent field-inspection tool. However, for routine bridge inspection, the removal of paint in all the areas to be inspected would be both difficult and expensive. It is quite likely that once the cracks open up enough to crack the paint, the dye penetrant could be used without removal of the paint. During this test, the paint was removed from all areas soon after the cracks had been detected ultrasonically, and no data were recorded that would indicate how large the crack in the base metal must be before it penetrates the paint layer.

Table 1. Ultrasonic crack measurements in bottom flange.

Inspection No.	Cycles (000s)	Crack Length at Indicated Section (mm)															
		2.1B		2.2B		2.3B		2.4B		6.1B		6.2B		6.3B		6.4B	
		N	S	N	S	N	S	N	S	N	S	N	S	N	S	N	S
1	0																
2	19.5							6[a]		5[a]			6[a]		6[a]	6[a]	6[a]
3	75.4							13[a]							13[a]	10[a]	13[a]
4	95.1	6[a]				6[a]		13[a]	6[a]	6[a]	6[a]		6[a]		13[a]	19[a]	18[a]
5	215.4	6[a]				6[a]		25[a]	6[a]	6[a]	6[a]		6[a]		13[a]	23[a]	25[a]
6	287.0	32[a]		33[a]	25	32[a]	38[a]	38[a]	38[a]	38[a]	38[a]	38[a]	38[a]	33[a]	38[a]	38[a]	25[a]
								6		20	15		27				
7	337.5	38[a]	38[a]	38[a]	38	38[a]	38[a]	38[a]	38[a]	47	46	14	27	38[a]	38[a]		38[a]
		18						6	6						6		6
8	348.7			38[a]						52	51		30				
9	360.9	22		6	38	38[a]	6	18	6	65	58	19	34	6	6		6
10	380.0	22		11	48					69	58	19	37				
11	402.1	22		15	53	38[a]	6	18	6	74	66	20	41	38	6		6
12	415.5	22		15	71	38[a]	6	18	6	85	83	20	44	38	6		6
13	422.5				71					89	83						
14	437.8				89												
15	447.9									119	108						
16	455.0				89					Failure							

Note: 1 mm = 0.0394 in; N = north side of flange; S = south side of flange.
[a]Crack between weld and end of plate; all other measurements are for cracks in base metal of girder flange.

Figure 9. Ultrasonic inspection of top flange.

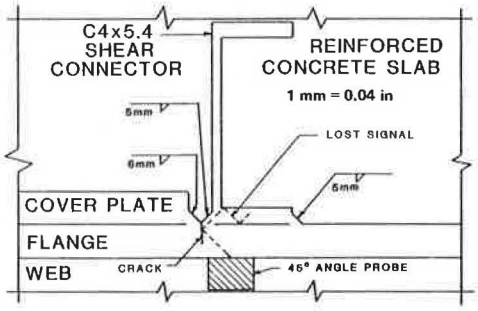

Radiography

Four sets of radiographs were taken by a commercial testing laboratory at 0, 95 000, 215 000, and 377 000 cycles of load. A set of radiographs included one 178x432-mm (7x17-in) film on each side of the bottom flange of each girder at sections 2 and 6. At 0 and 95 000 cycles, the set also included an identical series for the top flanges at sections 2 and 6. Of course, it was necessary to expose films of the top flanges through the reinforced concrete deck slab 152 mm (6 in) thick, and after two attempts it was concluded that interference from aggregate particles and reinforcing bars in the slab would obscure and prevent detection of any cracks that might be present in the top flange. Radiographs of the top flanges were discontinued after the second set. At 377 000 cycles, three additional films were shot along each side of each bottom flange at the center line of span 2.

All exposures were made with a 90-curie source of iridium 192 at a distance of 406 mm (16 in). Exposure times for the bottom flanges were 30 s and those for the top flanges were 15 min.

At 95 000 cycles, no cracks were indicated on the radiographic examination report, whereas the ultrasonic inspection indicated 10 cracks that varied from 6.4 to 19 mm (0.25 to 0.75 in) in length. At 215 000 cycles, the radiographic examination report indicated five cracks across the ends of the cover plates at the heel of the weld, whereas the ultrasonic inspection still indicated 10 cracks, two of which were 25 mm (1 in) long. However, four of the cracks that were detected radiographically were indicated to be only 6.4 mm (0.25 in) long by the ultrasonic inspection and had shown no growth since the previous ultrasonic inspection. The fifth crack had not been detected ultrasonically, and the radiograph showed that it had already penetrated the base metal of the bottom flange.

At 377 000 cycles, the radiographic examination report indicated 12 cracks in the critical regions of the bottom flanges, whereas the ultrasonic inspection indicated a total of 16 cracks. Again, there was no general trend in comparing the crack lengths as indicated by the two methods. For some cracks, the radiograph indicated the greater length, whereas for others the ultrasonic inspection indicated the greater length. The largest crack, which had been observed both ultrasonically and visually with the aid of a dye penetrant to be in excess of 64 mm in length, was not detected radiographically.

The special films exposed in the center span covered a region of the bottom flanges approximately 610 mm (2 ft) on either side of the center line of the bridge. No cracks were detected other than the one complete fracture of girder 2. Unfortunately, the region covered by these films was not quite long enough to cover the section in which the final fracture occurred approximately 93 000 cycles after these films had been exposed.

Radiographic inspection suffers from some of the same shortcomings that affect ultrasonic inspection. There tends to be a blind spot in the center of the flange directly opposite the web. It is also much easier to detect cracks that are oriented along a line from the film to the radiation source. This is because detection depends on the existence of a significant reduction in the density of material along the radiation line through the flange at the location of the crack. Thus, if the crack is not colinear with the radiation, the line intersects the crack for only a short length and there is little change in the total density of material along the line. Cracks can be detected only if they are open at the time the radiograph is taken.

Randomdec

The Randomdec technique of analyzing high-frequency

vibration signatures was employed as an inspection method by instrumenting the bridge with accelerometers at 24 stations. These stations were at the ends of the cover plates located on the top and bottom flanges of the girders in the two end spans. Two accelerometer stations were positioned in each bottom-flange region and one accelerometer station was positioned in each top-flange region. Detailed results of the Randomdec analysis are presented in a report by Reed and Cole (6).

CONCLUSIONS

Fatigue

Crack initiation, crack growth, and fracture are distinctly different phases of fatigue failure, and a given set of conditions may have significantly different effects on the initiation and growth phases. Thus it may not be possible to predict total fatigue life accurately on the basis of a simple relationship that involves only stress range and type of detail.

Both the initiation and growth phases are governed by the nature of stress cycles in a small zone around the tip of the crack. Mean stress in this zone has a significant effect on crack growth and possibly crack initiation, at least in those cases in which part of the stress cycle is in compression. These effects tend to be masked by high levels of tensile residual stress in tests of weldment details. Of course, these residual stresses are also present in prototype structures fabricated according to current practice, but the proportion of the cross section subjected to tensile stress is an important parameter, which may vary considerably from one structure to another. Finally, an understanding of the basic mechanisms of fatigue-crack initiation and growth may suggest changes in current practice that will improve the fatigue resistance of future structures. Additional research is needed to determine the exact stress conditions under which fatigue cracks begin as well as the conditions under which they propagate.

The premature failure of girder 2 at midspan points out the potential for fatigue-crack initiation resulting from the stamping of heat numbers in the flanges. Although this practice has been largely discontinued for rolled sections, it is still common practice to stamp identification numbers in plates during fabrication. If the final location of a stamped identification number is one of high repeated tensile stress, there is certainly a potential for fatigue-crack initiation. Consideration should be given to controlling the use of such identification stamps. The depth and sharpness of the stamp as well as its location are important factors.

Crack Detection

A conventional pulse-echo ultrasonic unit was the most reliable of the inspection methods. In those regions that were monitored regularly, no cracks are known to have grown to a length greater than 38 mm (1.5 in) without ultrasonic detection. However, undetected cracks did develop in regions that were not being monitored, and there is serious doubt whether those cracks would have been detected ultrasonically even if the region had been monitored.

Visual inspection appeared to be the second most reliable method of detection. Of course, cracks must penetrate the observed surface in order to be detected visually. Use of a dye penetrant significantly reduced the size of crack that could be detected visually.

Radiography was nearly as reliable as ultrasonic inspection in the regions in which it could be used. However, more than half the material to be inspected was inaccessible to radiography.

In some of the critical fatigue zones, the Randomdec method of detecting cracks produced crack predictions consistent with the ultrasonic results. However, the findings indicate that the methods of excitation employed in this study to generate the vibration signatures needed for the Randomdec analysis are not completely adequate for reliable crack detection.

The reliability of conventional ultrasonic techniques and radiography is sufficient to warrant the continued development of inspection programs that use these techniques along with visual inspection. However, it must be recognized that in the vicinity of complex connections, some cracks may become very large before they can be detected.

ACKNOWLEDGMENT

Research reported here was sponsored by the Missouri Highway Commission and the FHWA as a Highway Planning and Research Study. The bridge was made available by the U.S. Army Corps of Engineers, Memphis District. We gratefully acknowledge the help of numerous members of the Missouri Highway Department, FHWA, and Army Corps of Engineers. Robert E. Reed of Nielsen Engineering and Research, Inc., conducted the Randomdec study. Stanley T. Samborski III, former research assistant in civil engineering, is due special recognition for his work in collecting and reporting of the ultrasonic inspection and fatigue data.

REFERENCES

1. J.W. Fisher, K.H. Frank, M.A. Hirt, and B.M. McNamee. Effect of Weldments on the Fatigue Strength of Steel Beams. NCHRP, Rept. 102, 1970.
2. J.W. Fisher, P.A. Albrecht, B.T. Yen, D.J. Klingerman, and B.M. McNamee. Fatigue Strength of Steel Beams. NCHRP, Rept. 147, 1974.
3. Standard Specifications for Highway Bridges, 8th ed. American Association of State Highway Officials, Washington, DC, 1961.
4. H.J. Salane, R.C. Duffield, R.P. McBean, J.W. Baldwin, and T.V. Galambos. An Investigation of the Behavior of a Three-Span Composite Highway Bridge. Missouri Cooperative Highway Research Program, Rept. 71-5, Nov. 1971.
5. J.W. Baldwin, H.J. Salane, and R.C. Duffield. Fatigue Test of a Three-Span Composite Highway Bridge. Missouri Cooperative Highway Research Program, Rept. 73-1, June 1978.
6. R.E. Reed, Jr., and H.A. Cole, Jr. Randomdec: Mathematic Background and Application to Detection of Structural Deterioration in Bridges. FHWA, Rept. FHWA-RD-76-181, 1976.

Publication of this paper sponsored by Committee on Dynamics and Field Testing of Bridges.